

This article was downloaded by:

On: 25 January 2011

Access details: *Access Details: Free Access*

Publisher *Taylor & Francis*

Informa Ltd Registered in England and Wales Registered Number: 1072954 Registered office: Mortimer House, 37-41 Mortimer Street, London W1T 3JH, UK



Separation Science and Technology

Publication details, including instructions for authors and subscription information:

<http://www.informaworld.com/smpp/title~content=t713708471>

Nonspecific Effects of Ion Exchange and Hydrophobic Interaction Adsorption Processes

Joseph Korfhagen^a; Ana C. Dias-Cabral^b; Marvin E. Thrash^a

^a Department of Paper and Chemical Engineering, School of Engineering and Applied Science, Miami University, Oxford, OH, USA ^b Health Sciences Research Centre & Department of Chemistry, University of Beira Interior, Covilhã, Portugal

Online publication date: 15 September 2010

To cite this Article Korfhagen, Joseph , Dias-Cabral, Ana C. and Thrash, Marvin E.(2010) 'Nonspecific Effects of Ion Exchange and Hydrophobic Interaction Adsorption Processes', *Separation Science and Technology*, 45: 14, 2039 — 2050

To link to this Article: DOI: 10.1080/01496391003793876

URL: <http://dx.doi.org/10.1080/01496391003793876>

PLEASE SCROLL DOWN FOR ARTICLE

Full terms and conditions of use: <http://www.informaworld.com/terms-and-conditions-of-access.pdf>

This article may be used for research, teaching and private study purposes. Any substantial or systematic reproduction, re-distribution, re-selling, loan or sub-licensing, systematic supply or distribution in any form to anyone is expressly forbidden.

The publisher does not give any warranty express or implied or make any representation that the contents will be complete or accurate or up to date. The accuracy of any instructions, formulae and drug doses should be independently verified with primary sources. The publisher shall not be liable for any loss, actions, claims, proceedings, demand or costs or damages whatsoever or howsoever caused arising directly or indirectly in connection with or arising out of the use of this material.

Nonspecific Effects of Ion Exchange and Hydrophobic Interaction Adsorption Processes

Joseph Korfhagen,¹ Ana C. Dias-Cabral,² and Marvin E. Thrash¹

¹*Department of Paper and Chemical Engineering, School of Engineering and Applied Science, Miami University, Oxford, OH, USA*

²*Health Sciences Research Centre & Department of Chemistry, University of Beira Interior, Covilhã, Portugal*

This work illustrates the complexity of protein adsorption by ion exchange and hydrophobic interactions and the important role of nonspecific effects in the establishment of the adsorptive process. In ion exchange the interaction mechanism between chymotrypsinogen and lysozyme and two commercially available cation-exchange resins at different pH values and salt concentrations was studied. In hydrophobic interaction, the effect of temperature on the adsorption mechanism of bovine serum albumin onto epoxy-(CH₂)₄-sepharose was analyzed. In both cases observations have been made with respect to the results obtained from flow microcalorimetry. A direct correlation between the heat of adsorption data and isotherm measurements were observed.

Keywords flow micro-calorimetry; hydrophobic interaction; ion-exchange; isotherms; nonspecific interactions; protein adsorption

INTRODUCTION

It is well recognized that chromatography is a powerful technique for the separation and purification of biomolecules on a large process scale. Process chromatography has been implemented with a variety of mechanisms including ion-exchange (IE), affinity, partition, reversed phase, and hydrophobic interaction (HI). In each of these cases it is imperative, for economic reasons, to run the chromatographic process in the overloaded mode. Operation in the overloaded mode is considerably more complex than linear chromatography, and suitable models do not exist. Consequently, the prediction of separation behavior is generally unreliable. This is a major impediment in the design and implementation of scaled-up units. There is, therefore, considerable practical interest in developing a better understanding of the mechanisms underlying non-linear chromatography of biomolecules.

Received 30 November 2009; accepted 21 March 2010.

Address correspondence to Marvin E. Thrash, Ph.D., Department of Paper and Chemical Engineering, School of Engineering and Applied Science, Miami University, Oxford, Ohio 45056, USA. E-mail: thrashme@muohio.edu

Ion-exchange chromatography (IEC) and hydrophobic interaction chromatography (HIC) are popular techniques used in the purification of biological molecules such as proteins and peptides. These techniques are advantageous because most separations take place under mild conditions and the proteins usually maintain their activity throughout the process (1,2). In typical IEC the polarity of the adsorbent's surface charge is opposite to that of the target protein(s) in the mobile phase (1). In HIC applications the interaction between the protein and the adsorbent is usually facilitated by the presence of a chaotropic salt such as ammonium chloride or ammonium sulfate (2). Although IEC and HIC adsorbents serve their purpose extremely well, the main challenge with any chromatographic technique is predicting the adsorptive behavior of the biomolecules to be purified for any range of concentrations, especially in mass overloaded conditions. Modeling protein adsorption in IEC and HIC for the purpose of predicting protein isotherms under these conditions is indeed a challenging task. The primary reason for this is that more interactions between the protein and the adsorbent can occur than the expected primary interaction. For example, water-release is a phenomena usually associated with HIC (2), however, this phenomena can also be present in ion exchange applications. The release of water from the contact surface of the protein and the adsorbent can significantly influence protein adsorptive behavior in IEC applications (3). To address these additional interactions a number of models have been developed over the years. The Steric Mass Action Model (4), the Non-Ideal Surface Solution Model (5,6) are examples of mass actions models that utilize a correction factor to account for non-ideal interactions. In addition to these methods, fundamental models based on the solution of the Poisson Boltzmann equation are also utilized (7,8). More recently the Available Area Model (9) was developed to simulate protein isotherms. Each of the models account for specific events associated with the adsorption process. The Steric mass

action model accounts for the effect of steric hindrance associated with protein adsorption. The non-ideal surface solution model accounts for non-ideal surface effects such as repulsion between surface proteins with the same charge. Variations of the Poisson Boltzmann model account for the free energy contribution associated with specific events such as electrostatics, vander Waals interactions, etc. and, the Available Area Isotherm accounts for geometrical exclusion due to already adsorbed proteins. In order for these models or any other model to accurately predict the adsorptive behavior of proteins, the driving forces associated with protein adsorption must be identified and mathematically quantified. If not, then erroneous results will be produced. For example, in the case of ion-exchange, a favorable interaction (i.e., release of energy) is expected when two oppositely charged surfaces come into contact; however, in some IEC applications, calorimetry has given results contrary to this expectation. Gill et al. (10), Hughes and Bowen (11), Raje and Pinto (6), and Thrash et al. (3,12,13), have all shown that the adsorption of proteins onto ion-exchange surfaces can be endothermic. In these applications driving forces in addition to electrostatics must be present. Consequently if any of these systems are to be modeled, all of the adsorptive driving forces must be properly quantified. For these specific examples, the adsorption of proteins has to be driven by entropic forces since the Gibbs free energy (ΔG) has to be negative. Endothermic heats can arise from a number of sources such as repulsive interactions between surface molecules, repulsive interactions between hydrophobic groups on the protein surface and hydrophilic moieties on the adsorbent surface, repulsive interactions between charged groups on the protein's surface and charged surface sites on the adsorbent possessing the same charge, release of water from the adsorbent surface and the contact surface of the protein, conformational changes in the protein's three-dimensional structure, reorientation of surface proteins or some combination of these effects (6,11). For the adsorption of Bovine Serum Albumin (BSA) onto some anion exchangers it has been suggested that dehydration of the sorbent and protein contact surface may in part be responsible for the production of endothermic heats under conditions where protein conformational changes are not expected (13,14). With regard to HIC it is generally known that surface phase changes in entropy are extremely important (2). However, it was also demonstrated (15–18) that under overloaded conditions, the adsorption enthalpy can be positive and/or negative depending on mobile phase conditions (salt type and concentration and support ligand type and length). The overall process may be either entropically driven, enthalpically driven, or both entropically and enthalpically driven.

In this paper the role of nonspecific adsorptive driving forces was investigated for lysozyme, chymotrypsinogen,

and BSA. Specifically the effect of pH on the adsorption of chymotrypsinogen, and lysozyme was studied using cation exchange adsorbents (carboxymethyl cellulose and titanium oxide) and the effect of temperature on the hydrophobic interaction adsorption of bovine serum albumin onto epoxy – $(CH_2)_4$ – Sepharose was analyzed. To study equilibrium behavior under linear and overloaded conditions, protein adsorption isotherms were measured and flow microcalorimetry was used to study the energetics of adsorption under overloaded (nonlinear) conditions.

EXPERIMENTAL

Materials and Apparatus

Chymotrypsinogen, lysozyme, and BSA were purchased from Sigma (St. Louis, MO, USA) and used without further purification. The adsorbents used in this study were carboxymethyl cellulose (CMC), titanium oxide, and epoxy – $(CH_2)_4$ – Sepharose. CMC is a strong cation exchange material with a negative surface charge. This adsorbent was purchased from the Whatman Company. The titanium oxide (also a strong cation exchanger) was purchased from Sigma (St. Louis MO, USA). Ion-exchange adsorption studies were conducted at pH 8 and pH 5. The solution pH was adjusted to 5 using piperazine (MW = 86) and 8 using trizma base (MW = 121). The concentration for each buffer was 20 mM. Sodium chloride (MW = 58.44) was the only modulator used in the ion-exchange experiments. Sodium chloride and the buffers were purchased from the Fisher Scientific Company (Hanover Park, IL., USA). The HIC support was a Sepharose derivative synthesized by covalent immobilization of the ligand 1,4-butandiol diglycidyl ether on Sepharose CL-6B purchased from Pharmacia BioTech Europe. The synthesis procedure has been described in detail elsewhere (19). A 10 mM sodium phosphate buffer (pH 7), which consisted of a mixture of equimolar dibasic and monobasic sodium phosphate from Aldrich (Steinheim, Germany), was used for all hydrophobic interaction experiments. Analytical-grade ammonium sulfate from Aldrich (Steinheim, Germany) was used as the modulator.

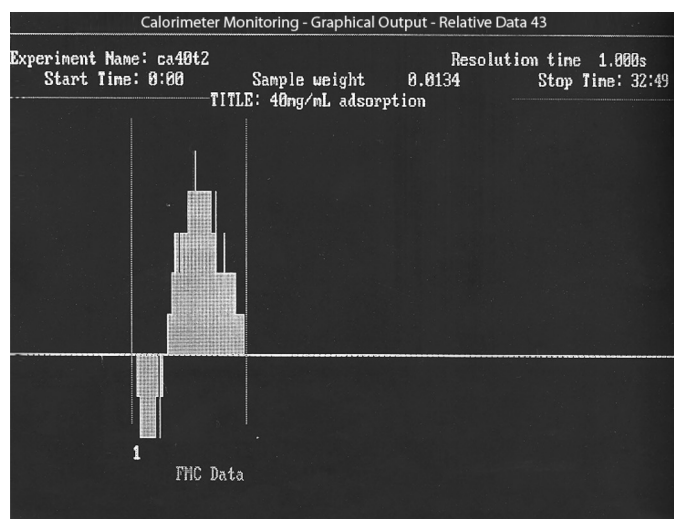
Flow Microcalorimetry

The Flow MicroCalorimeter (FMC) (Gilson Instruments, Westerville, OH., USA) is operated similar to a liquid chromatograph. The column (or cell) volume is 0.171 mL and is interfaced with two highly sensitive thermistors. The FMC is capable of detecting small temperature changes within the cell that are associated with the adsorption of an analyte onto the surface of a particular adsorbent. The flow rate through the cell is controlled by precision syringe micropumps. A block heater is used to monitor and control the cell temperature. As in a chromatograph, the FMC is equipped with a configurable injection loop to

accommodate different injection volumes. The effluent was collected and analyzed with a UV Spectrophotometer (Milton Roy, Rochester NY). The FMC is initially filled with a specified volume of adsorbent. The next step is usually the evacuation of the cell; however, in these experiments the adsorbent was wetted with the mobile phase or carrier fluid. Following wetting, the syringe pumps are turned on and the adsorbent is equilibrated with the carrier solution at a flow rate of 1.5 mL/h for the ion-exchange adsorbent and 3.33 mL/h for the hydrophobic interaction adsorbent. When the system has reached thermal equilibrium, the sample (protein dissolved in the carrier fluid) is loaded into a 0.77 mL (ion-exchange adsorbent) or 91 μ L (hydrophobic interaction adsorbent) injection loop, and introduced into the cell by switching a multiport valve. The adsorption of the sample onto an adsorbent surface causes a change in cell temperature, which is converted to a heat signal by the FMC through an experimentally determined calibration factor. (the calibration factor was obtained using an electrical impulse of 0.030 J). Heat evolution or absorption during the adsorption/desorption processes is indicated by changes in potential (imbalance in the thermister bridge in which two thermistors measure temperature changes in the adsorbent bed) recorded in μ Volt by an analog recorder and in digital form (Fig. 1a) in computer memory. These data, once processed by Caldos 3 (a program that acquires, stores, presents, annotates, processes, calibrates, and manages data for the entire FMC system), yield enthalpy information which characterizes the particular interaction between the adsorbate and the adsorbent (Fig. 1b). Once the mass in the effluent is quantified with the spectrophotometer, a simple mass balance is performed to determine the quantity of sample adsorbed. From these data the specific heat of adsorption is calculated. Two replicated studies were done at each experimental condition, which give concordant results.

Isotherms

Protein isotherms were measured at selected pH, modulator concentrations, and temperature using a batch method. The adsorbent (carboxymethyl cellulose, titanium oxide, or epoxy - $(CH_2)_4$ - Sepharose) was first weighed into individual test tubes, and then a measured volume of protein solution of a known pH, salt, and protein concentration was added. The test tubes were then sealed with parafilm, placed in a shaker, and agitated at 200 rpm for 24 h at the selected temperature. Preliminary experiments have established that equilibrium is effectively reached in 24 h. After equilibration, the slurry solution was allowed to settle for 30 min and a sample of the supernatant was removed with a filter (0.45 μ m) syringe. The absorbance of the filtrate was measured at 280 nm, with a UV spectrophotometer (Milton Roy, Rochester NY or Amersham Biosciences, Uppsala, Sweden) to obtain the equilibrium



(a)

Data from channel 1

Input calibration factor is 12943.8220

Data from channel 1

Peak 1:	Start time	End time	Duration (min)	Energy (mJ)
Endothermic	5:48	7:33	1:45	-0.0095
Exothermic	7:33	11:19	3:46	0.0470

(b)

FIG. 1. (a) Digital output of example heat signal using Caldos software (BSA adsorption onto epoxy - $(CH_2)_4$ - Sepharose [$(1.0\text{ M } (NH_4)_2SO_4$, phosphate buffer, pH 7.0, 296 K, protein loading: 40 mg mL^{-1} (91 μ L)] and (b) Example FMC heat of adsorption data.

solution concentration. The equilibrium distribution was calculated from a mass balance.

Zeta Potential Measurements

In order to measure the zeta potential of titanium oxide, a Zeta-Meter System 4.0 was purchased from Zeta-Meter, Inc. based in Staunton, VA. To start, 0.48 g of titanium oxide was weighed out and dissolved in 300 mL of buffer (20 mM) adjusted to the desired pH. We then cycled the solution from the beaker through an electrophoresis cell using the automatic transfer component of the machine. Two electrodes were connected to the cell, a positive electrode to the Molybdenum anode and a negative electrode to the Platinum Cathode. This caused a DC voltage in the cell, making the charged colloids move towards the anode at velocities relative to their surface charges. Using a high powered microscope, we proceeded to track 100 different colloids traveling along the stationary layer line, and the machine formulated an average zeta potential based on the electrophoresis mobility results. The solution was recycled through the cell after every five colloids tracked.

This process was repeated in a different buffer adjusted to pH 5. The zeta potential of carboxymethyl cellulose was found using the same process except with 1.44 g of carboxymethyl cellulose in 300 mL of an aqueous buffer.

RESULTS AND DISCUSSION

The isotherms for chymotrypsinogen at pH 8 and 25°C are presented in Fig. 2. It can be observed that the affinity between the protein and the adsorbent is very weak in the initial stages; however, the surface concentration appears to increase in a nonlinear manner as the solution concentration of chymotrypsinogen increases, thus producing an isotherm with an upward concave shape. In experiments conducted by Tung and Steiner (20) on chymotrypsinogen, it was observed that at pH 8 and above, this protein formed dimers, trimers, tetramers, and other types of aggregates in solutions with low ionic strengths. It was also shown that chymotrypsinogen aggregation increases with the concentration of protein (20). When the concentration of protein increases the size of the protein aggregates also increases and hence this behavior leads to the adsorption of larger clusters and higher concentrations of protein on the surface. At higher protein concentrations the observed nonlinear increases in surface concentration may also be attributed to the formation of even larger aggregates on the surface of the adsorbent possibly leading to multilayer formation resulting from interactions between adsorbed aggregates and aggregates in solution. These types of isotherms can be also found when adsorbate-adsorbate interactions are present on the adsorbent surface (21). From Fig. 2 it can also be seen that the surface concentration of protein is the greatest in the absence of salt. In this experiment, the maximum surface concentration was observed to be slightly greater than 200 mg of protein per gram of adsorbent for a chymotrypsinogen solution concentration of approximately 12 mg/mL. When the sodium chloride concentration is increased to 50 mM, the shape of the isotherm did not change significantly; however, at the same chymotrypsinogen solution concentration where the maximum surface concentration obtained was observed, its value is reduced to approximately 40 mg/g. The affinity

between the protein and the adsorbent is still very weak particularly when the protein concentration is low. When the salt concentration is raised to 100 mM, the surface protein concentration that corresponds to a solution concentration of 12 mg/mL is not significantly different from the results obtained at 50 mM. Tung and Steiner (20) also showed in their study that aggregate formation is reduced but not totally eliminated as the salt concentration is increased. Since aggregate formation is greater in the absence of salt, protein adsorption is occurring in clusters instead of individual molecules. The isotherms presented in Fig. 2 show that in the absence of salt the surface concentration of protein is greatest. This is likely due to the adsorption of large clusters. As the salt concentration is increased aggregate formation is reduced leading to the adsorption of smaller clusters which in turn produces lower surface concentrations.

The charge of chymotrypsinogen at pH 8 is +3 (Table 1). The isoelectric point of chymotrypsinogen occurs at pH 9. At pH 8 the protein is not fully charged and the charge density (charge/external protein surface area) is only 1 $\mu\text{C}/\text{cm}^2$. Since the surface charge density is low, binding mechanisms besides ion-exchange, as previously discussed, seems to be influencing the adsorptive behavior of the protein.

Chymotrypsinogen isotherms were also measured at pH 5. The results are shown in Figs. 3a, 3b, and 3c. Figure 3a shows the adsorption of chymotrypsinogen in the absence of sodium chloride. Note that in the absence of salt the overall shape of the isotherm is different from that observed at pH 8. Here the isotherm has a downward concave shape that is similar to a Type I Langmuir isotherm (21). At the lower pH, the maximum protein concentration on the surface for a chymotrypsinogen solution concentration of approximately 7 mg/mL was observed to be approximately 400 mg/g in the absence of salt. As shown in Fig. 3b, a significant reduction in protein surface concentration was observed when the salt concentration was raised to 50 mM. The overall shape of the isotherm became more linear and the observed maximum protein concentration on the adsorbent at the chymotrypsinogen solution concentration of approximately 7 mg/mL was reduced to approximately 80 mg/g. Figure 3b also shows that increasing the salt concentration to 100 mM did not produce an isotherm that was significantly different from the results produced at 50 mM. At 200 mM salt concentration (Fig. 3c), the surface concentration of protein is significantly reduced. The surface concentration of protein never exceeded 25 mg/g at 200 mM salt. As expected, the surface concentration of protein is inversely proportional to the salt concentration. This is because the salt effectively screens the electrostatic interactions between the protein and the adsorbent (1). This phenomenon is common in ion exchange applications. Moreover, at pH 5, the overall isotherm shape has changed becoming concave downwards.

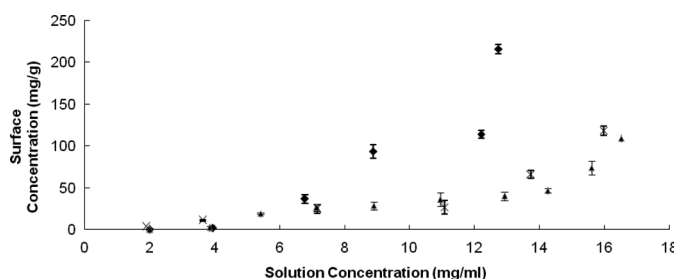


FIG. 2. Chymotrypsinogen - carboxymethyl cellulose isotherms at pH 8 and 25°C, \blacklozenge - 0 mM NaCl; \blacktriangle - 50 mM NaCl; \times - 100 mM NaCl (1).

TABLE 1

Protein charge and charge density (The charge on lysozyme was calculated from data published by Oberholzer, Wagner and Lenhoff (22,23). The charge on chymotrypsinogen was estimated from reference (24). To calculate the surface charge densities the surface areas of each protein were calculated. The molecular radius of lysozyme and chymotrypsinogen were assumed to be 15.6 angstroms 19.3 angstroms respectively (25) in the surface area calculations.)

	pH 8	pH 5
Chymotrypsinogen charge	+3	+6
Chymotrypsinogen charge density ($\mu\text{C}/\text{cm}^2$)	+1.0	+2.0
Lysozyme charge	+7	+11
Lysozyme charge density ($\mu\text{C}/\text{cm}^2$)	+3.66	+5.7

As shown in Table 1, the net charge on chymotrypsinogen is approximately +6 at pH 5. At pH 5 the protein possesses a greater charge and thus the charge density (surface potential/external protein surface area) is higher. In this case the charge density is $2.0 \mu\text{C}/\text{cm}^2$. The shape of the isotherms at pH 5 indicates or at least suggests the adsorptive mechanism is different. The mechanism of ion exchange may be more dominant under these experimental

conditions, as the self-association of chymotrypsinogen seems not to be present. Tung and Steiner (20) found that for a particular electrolyte level (independent of its characteristics) and protein concentration, the degree of association decreased with decreasing pH below pH 8, becoming negligible below pH 6.

Heat of adsorption data for chymotrypsinogen (20 mg/ml) was collected in an attempt to further analyze these results. Measurements were taken in the absence of salt to ensure that the heat signal was strong enough to be detected. At pH 8 the heat of adsorption of chymotrypsinogen was determined to be endothermic. The measured value of ΔH at pH 8 was determined to be 17 Kcal/mole (Table 2). At pH 5 the heat of adsorption of chymotrypsinogen was determined to be exothermic, indicating the presence of favorable interactions. The actual value of ΔH was determined to be -24 Kcal/mole at the lower pH (Table 2). These data support the possibility that the ion exchange mechanism may indeed be more dominant at the lower pH. Moreover, the fact that the heat of adsorption was endothermic at pH 8 and exothermic at pH 5 underscores the presence of different adsorptive mechanisms at each pH. This assumption is further supported by the different isotherms shapes at each pH. For adsorption to occur the Gibbs free energy contribution (ΔG) must be negative. Note the Gibbs free energy has both an enthalpic contribution (ΔH) and an entropic contribution ($T\Delta S$). Since the measured value of ΔH was positive at pH 8, it is reasonable to conclude that protein adsorption has to be entropically driven under these

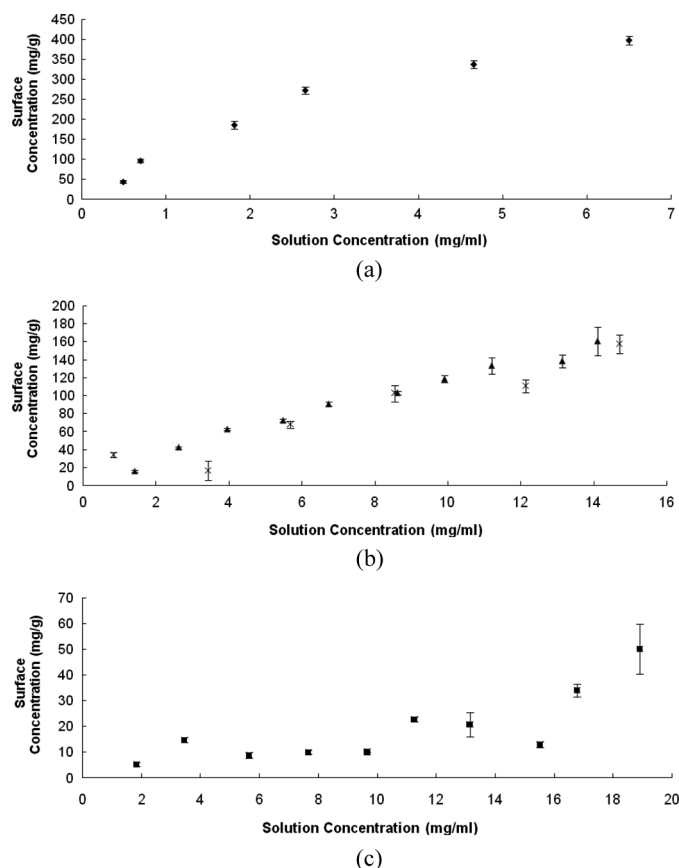


FIG. 3. Chymotrypsinogen - carboxymethyl cellulose isotherms at pH 5 and 25°C. (a) In the absence of salt; (b) \blacktriangle - 50 mM NaCl; \times - 100 mM NaCl; (c) In the presence of 200 mM NaCl (1).

TABLE 2
Heat of adsorption data collected for chymotrypsinogen and lysozyme adsorption onto carboxymethyl cellulose

	pH 8	pH 5
Chymotrypsinogen (kcal/mole)	+17	-24
Lysozyme (kcal/mole)	-17	-5

conditions. As previously stated, a possible explanation for this is that when the charge density of chymotrypsinogen is lower, driving forces other than ion exchange are more prominent. These non-specific driving forces may include entropic contributions such as re-orientation or conformational changes in the protein structure, multi-layer formation (as previously discussed), and/or release of water molecules from the contact surface of the protein and the adsorbent. In order to decide which of these processes are involved, other studies should be done like the dependence of adsorptive heats on the surface concentration. Unfortunately because of a weak heat signal at lower surface concentrations of protein, that was not possible in this study. The enthalpic contribution from all these events will produce endothermic heats while simultaneously increasing the entropy of the process. Proteins are highly structured entities. Their activity or biological function depends on their structural integrity. An entropy gain is expected when the protein's structure loses order. Likewise water molecules attached to the exterior hydrophobic patches of a protein in solution have been reported to exist in highly ordered arrangements (26). Upon adsorption these water molecules are released into the surrounding environment. In this process, the release of water molecules bound to the contact surface of the protein and the adsorbent experience a loss in order thus resulting in an increase in entropy (11,13,26-28). As the charge density of the protein is increased at the lower pH, electrostatic driving forces become more pronounced.

With respect to chymotrypsinogen, it is clear that the adsorptive driving forces are different at each pH. This difference is reflected in the calorimetry results and the isotherm plots. In order to simulate any of these isotherms a modeler must have a reasonable understanding of what adsorptive events are taking place such as water release, interaction between surface proteins, etc. These types of results underscore the challenges associated with the development of robust isotherm models.

Isotherm measurements studying the adsorption of lysozyme onto carboxymethyl cellulose were also collected. These measurements were taken at pH 8 and pH 5 at 25°C. The data collected at pH 8 is presented in Fig. 4a and 4b. As shown in Fig. 4a, the adsorption capacity of lysozyme was highest in the absence of salt at pH 8. The maximum surface concentration under these conditions was observed to be approximately 600 mg/g at a solution concentration of approximately 0.8 mg/mL. Unlike chymotrypsinogen the initial slope of the isotherm in the linear region is very steep in the absence of salt, thus indicating a very strong affinity between lysozyme and the adsorbent. When the salt concentration is raised to 50 mM (Fig. 4a), the maximum surface concentration is still close to 600 mg/g. This shows that the screening effect of the salt is minimal. At 100 mM salt concentration (Fig. 4a) the

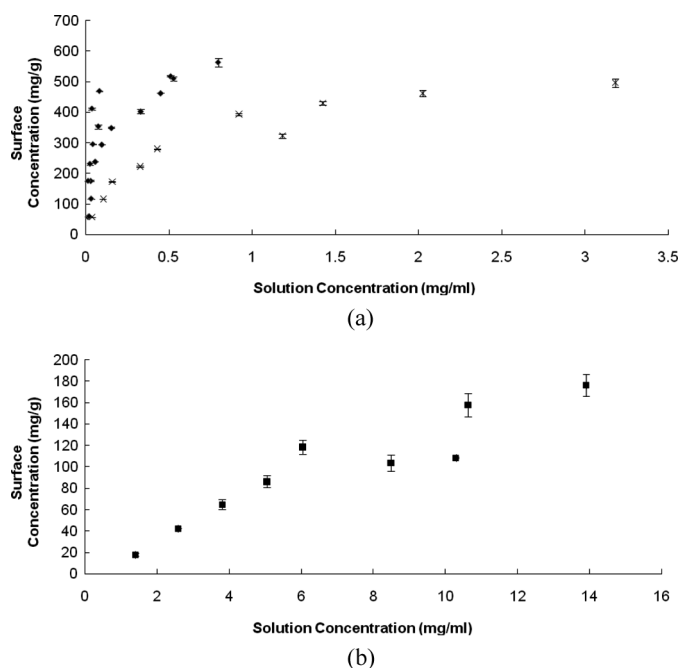


FIG. 4. Lysozyme - carboxymethyl cellulose isotherms at pH 8 and 25°C. (a) \blacklozenge – in the absence of salt; \blacktriangle – 50 mM NaCl; \times – 100 mM NaCl; (b) 200 mM NaCl (1).

maximum surface concentration is observed to be lower. Under these conditions the maximum surface concentration of lysozyme, obtained at a solution concentration of approximately 3 mg/mL has fallen to approximately 500 mg/g. The distribution coefficient in the linear region also appears to be lower in the presence of 100 mM NaCl. At 200 mM NaCl (Fig. 4b) the maximum surface concentration of protein has been reduced to approximately 200 mg/g and has been obtained at a solution concentration of approximately 14 mg/mL. Moreover, the shape of the isotherm appears to be more linear. This is to be expected considering the salt effect on ion-exchange interactions (1).

As shown in Table 1 the net charge of lysozyme at pH 8 is approximately +7. The isoelectric point of lysozyme occurs at pH 10.5. At pH 8 the lysozyme is not fully charged and the charge density of lysozyme was calculated to be 3.66 μ C/cm². At the higher pH, the charge density of lysozyme is greater than chymotrypsinogen's charge density. This difference in electrostatic properties could possibly represent a key factor as to why the adsorptive behavior of lysozyme is significantly different from the adsorptive behavior of chymotrypsinogen at the higher pH. Although lysozyme has also a tendency to form polymers, between pH 5 and 9 it occurs predominantly as a dimer, forming only higher polymers above pH 9 (29).

Lysozyme adsorption was also studied at pH 5. The results are shown in Fig. 5. As expected, the highest surface

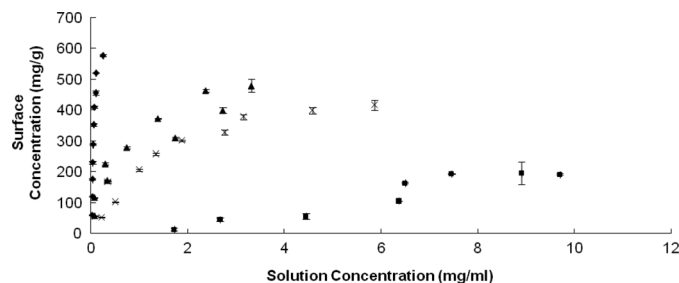


FIG. 5. Lysozyme - carboxymethyl cellulose isotherms at pH 5 and 25°C. \blacklozenge - In the absence of salt. \blacktriangle - 50 mM NaCl; \times - 100 mM NaCl. \blacksquare - 200 mM NaCl (1).

concentration of lysozyme was observed in the absence of salt. As shown in Fig. 5 the maximum surface concentration of protein is approximately 600 mg/g. This is consistent with the data collected at pH 8 shown in Fig. 4a. The only observable difference between the data at pH 8 and pH 5 in the absence of salt is a slight difference in the distribution coefficients of the linear region of the isotherms. When the salt concentration is increased to 50 mM the maximum surface concentration of lysozyme is reduced to approximately 500 mg/g and is obtained at a solution concentration of approximately 4 mg/mL. Moreover, the distribution coefficient of lysozyme in the linear region of the isotherm is less under these conditions. As the salt concentration is further increased to 100 mM, the maximum surface concentration of lysozyme has been reduced to 400 mg/g (obtained at a solution concentration of approximately 6 mg/mL). The isotherm plot for lysozyme in the presence of 200 mM NaCl is not as non-linear as the other plots and shows that the maximum surface concentration has been reduced to approximately 200 mg/g (obtained at a solution concentration of approximately 9 mg/mL).

As seen in Table 1 the net charge on lysozyme at pH 5 is greater and thus the charge density is also greater. From this data it is reasonable to expect the ion-exchange mechanism to be more prominent under these conditions; however, the protein surface concentrations in the overloaded region of the isotherm (in presence of salt) appears to be slightly lower when compared to the data collected at pH 8. Calorimetry was used to further investigate this.

Heat of adsorption measurements were also taken for lysozyme (20 mg/mL) adsorption onto carboxymethyl cellulose at pH 8 and pH 5. As with chymotrypsinogen, these measurements were also taken in the absence of salt to ensure the adsorptive heats were large enough to be detected by the temperature sensors inside the flow cell. The heat of adsorption was determined to be -17 kcal/mol at pH 8 and -7 kcal/mol at pH 5 (Table 2). ΔH was exothermic under both experimental conditions. Exothermic heats are an indication that the ion-exchange

mechanism may be more pronounced for lysozyme. The charge density for lysozyme was greater than the charge density for chymotrypsinogen in the experimental conditions used in this study. Although the charge density for lysozyme was greater at pH 5, the magnitude of the ΔH was lower at pH 5. A possible explanation for this may be due to the presence of repulsive interactions between surface proteins under overloaded conditions. Repulsion arises when molecules of like charge are in close proximity to each other. The effect has been discussed in detail by Raje and Pinto (6). This could be a possible explanation for the reduction in the initial rise of the isotherms observed at pH 5; however, calorimetry measurements with greater heat signal detection capability are needed to verify this hypothesis in the presence of salt and in the absence of salt.

In order to study the effect of the carbonaceous stationary phase of the CMC on the adsorption of chymotrypsinogen and lysozyme, the adsorption of these proteins onto titanium oxide (TiO_2) was also analyzed. Like CMC, TiO_2 also possesses a strong net negative charge. The zeta potentials of the TiO_2 particles and of CMC were measured to be approximately, -51 mV and -60 mV respectively in the absence of salt. Moreover, the zeta potential of titanium oxide of CMC did not significantly change with the pH. These data were consistent with other prior studies (30,31). Isotherm measurements on TiO_2 were done in the absence of salt at pH 8 for lysozyme and at pH 5 for lysozyme and chymotrypsinogen (Fig. 6a). In Fig. 6a we change the units of surface concentration to mg/cm^2 . We normalized adsorption capacity in terms of the surface area to compare the differences between the two adsorbents. Since lysozyme is considered a rigid protein we estimated the surface area of CMC to be $348 \text{ m}^2/\text{g}$. This value was estimated from protein adsorption data provided by the supplier of the CMC adsorbent. BET measurements determined the surface area of the titanium oxide to be $149 \text{ m}^2/\text{g}$. In every studied case the shape of the isotherms in the presence of the metal oxide is less rectangular than the isotherms measured with CMC, suggesting that the isotherm overloaded region has not been reached at the equilibrium solution concentrations analyzed. By assuming chymotrypsinogen as a sphere with a radius of 19.6 angstroms, the theoretical maximum surface concentration will be approximately 297 mg/g or 0.00020 mg/cm^2 for monolayer coverage on titanium oxide. The theoretical maximum attainable surface concentration for lysozyme adsorption on titanium oxide was estimated to be 488 mg/g or 0.00033 mg/cm^2 assuming lysozyme as a sphere with a radius of 15 angstroms. In each of the analyzed cases (Fig. 6a) the experimentally observed surface concentration of protein is far less than the theoretical maximum. Also, the isotherms obtained for the adsorption of chymotrypsinogen onto titanium oxide at pH 5 and for

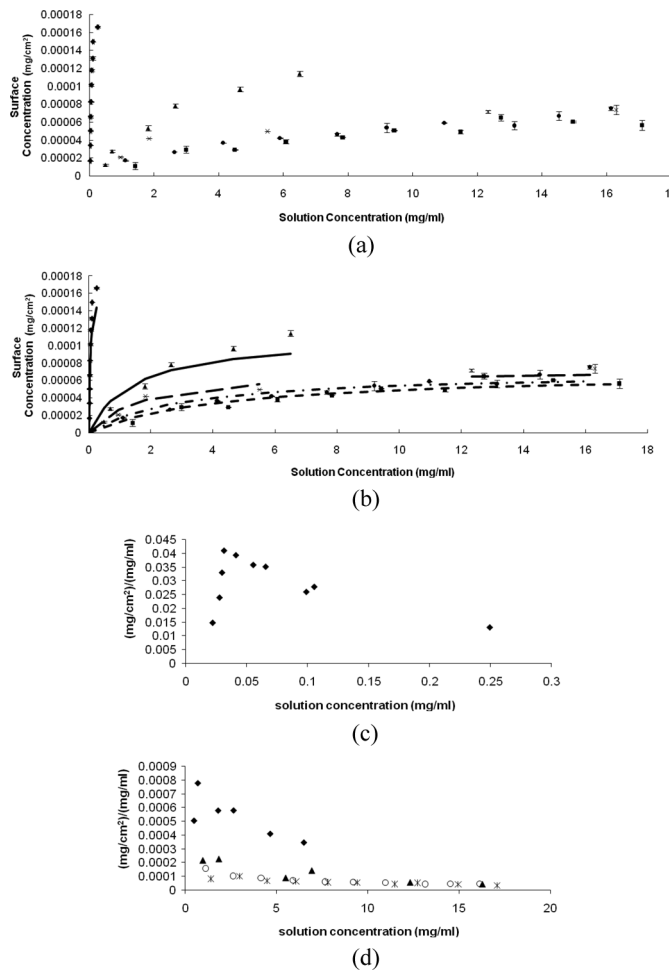


FIG. 6. (a) Protein - Adsorbent Isotherms in the absence of salt, at 25°C. ♦ - lysozyme-CMC, pH 5; ▲ - chymotrypsinogen-CMC, pH 5; x - chymotrypsinogen-TiO₂, pH 5, ■ - lysozyme-TiO₂, pH 5; ▲ - lysozyme-TiO₂, pH 8 (1); (b) Languir isotherm plots using parameters in Table 3; (c) Scatchard plot of lysozyme on CMC at pH 5; (d) Scatchard plot of lysozyme on TiO₂ and chymotrypsinogen on CMC and TiO₂. ♦ - chymotrypsinogen-CMC at pH 5, ▲ - chymotrypsinogen-CMC, pH 5, o-lysozyme-TiO₂ pH 5, * - lysozyme-TiO₂ pH 8.

the adsorption of lysozyme onto titanium oxide at pH 8 and pH 5 are similar. This is to be expected, if ion exchange is the only mechanism present. Note the charge is similar for the two proteins (6 for chymotrypsinogen and 7 for lysozyme (Table 1)) and the zeta potential of titanium oxide is a weak function of pH (30).

Upon comparison of the two adsorbents, the surface concentration of protein is always greater on CMC than on titanium oxide. The surface concentration of chymotrypsinogen on CMC, at pH of 5, for a solution concentration of approximately 7 mg/mL, approached 400 mg/g or 0.000114 mg/cm² (Fig. 6a) while on the titanium oxide the surface concentration was closer to 110 mg/g or 0.000074 mg/cm² (Fig. 6a). The same tendency is observed for the adsorption of lysozyme onto CMC and titanium

oxide at each pH (Figs. 3a and 5), indicating for lysozyme - TiO₂ a lower affinity between the protein and the adsorbent surface. If ion-exchange is the primary adsorptive driving force it is reasonable to expect the protein to populate the surface of TiO₂ as it does CMC, however, this effect was not observed. As previously stated, at pH 5 the potential of the CMC and the titanium is negative and the protein has a strong net positive charge (Table 1). The primary difference between the two supports is the absence of a carbon based stationary phase on the surface of the titanium oxide. This may be the primary reason for the striking difference in the isotherm results. Moreover, the difference in surface concentration between the two adsorbents may also be the result of a stronger entropic driving force associated with the carbonaceous stationary phase of the CMC. We attempted to measure the heat of adsorption of chymotrypsinogen and lysozyme on TiO₂; however, the low surface concentration produced a weak signal that was not discernable. In spite of this, the TiO₂ isotherm results clearly indicate the presence of adsorptive driving forces other than ion-exchange when either protein binds to the surface of CMC. The release of water from the contact surface of the protein and carbonaceous moieties on the CMC surface and/or structural rearrangements of the protein on the surface of CMC may be contributing events that entropically drive adsorption. The free energy contribution associated with these events increases the favorability of adsorption. In prior studies investigating BSA adsorption onto an anion exchange surface, it has been shown that the free energy contribution arising from water-release is greater than that associated with the free energy contribution arising from electrostatics (13).

Plots drawn according to the Langmuir (35) isotherm model (Eq. 1) are shown in Fig. 6b.

$$q = \frac{q_m K C}{1 + K C} \quad (1)$$

The parameters q_m and K are shown in Table 3. The maximum adsorption capacity q_m was estimated from the isotherm data and K was a fitted parameter. Scatchard

TABLE 3
Langmuir isotherm parameters used in Fig. 6b

	q_m (mg/cm ²)	K (cm ³ /mg)
Lysozyme-CMC at pH 5	0.00017	21.63
Chymotrypsinogen-CMC at pH 5	0.00011	0.709
Chymotrypsinogen-TiO ₂ at pH 5	0.000074	0.572
Lysozyme-TiO ₂ at pH 5	0.000070	0.331
Lysozyme TiO ₂ at pH 8	0.000070	0.234

(36) plots for the isotherms in Fig. 6a are shown in Figs. 6c and 6d. The nonlinear shape of the protein-CMC plots in Figs. 6c and 6d indicate the presence of the different adsorption mechanisms while the plots for protein adsorption on titanium oxide displayed less variation. A key assumption of the Langmuir isotherm is that all adsorption sites are energetically equivalent. The presence of multiple mechanisms as indicated by the Scatchard plots nullifies this assumption. Alternative models such as the Mass Action model⁴ or the Colloidal model⁸ may be more appropriate. These models do however require additional fitting parameters which could not be determined for our study because a wider range of salt concentration is needed. Nonetheless, our results suggest the higher protein adsorption capacity on CMC may be the result of a cumulative effect of ion-exchange working in concert with additional adsorptive driving forces.

With regard to HIC, as stated in the introduction, behavior different from the expected is observed under overloaded conditions (15–18). Prior work has shown the existence of nonspecific effects in the adsorption of BSA onto epoxy – (CH₂)₄ – sepharose in the presence of 1.0 M (NH₄)₂SO₄ at 296 K (15). It was shown that under overloaded conditions a typical calorimetry signal has two overlapping peaks, an endothermic peak and an exothermic peak. Moreover, at high protein loadings the process appeared to be driven both by enthalpy and entropy. These results were quantitatively correlated to the adsorption isotherm. Specifically the exothermic heats were observed in the region of the isotherm where the surface concentration exhibits a rapid increase. This behavior has been argued to be consistent with re-orientation and/or change in conformation of the adsorbed proteins. The exothermic heat of adsorption would increase, due to attractive interactions between adsorbed molecules, when re-orientation/reconfiguration first occurs and would decrease as a new monolayer capacity is reached. Upon comparison with the calorimetry results for our ion-exchange studies, overlapping peaks were not present. Single exothermic or endothermic peaks were observed for lysozyme and chymotrypsinogen. At pH of 5 the adsorption of lysozyme and chymotrypsinogen were enthalpically driven. Adsorption was only driven by entropy for chymotrypsinogen at pH of 8. It can also be observed that, compared with ion-exchange, lower values of ΔH were obtained for HIC studies (Fig. 7 and reference 15). The differences stem from the different protein/adsorbent systems studied, emphasizing the widely different behaviors that systems can manifest. The strength of interaction may justify the observed values. We have previously observed the influence of different types of hydrophobic supports (17,18) and salt (17) on the adsorption of BSA, and in some cases ΔH values on the order of magnitude of the ones obtained in ion-exchange were observed.

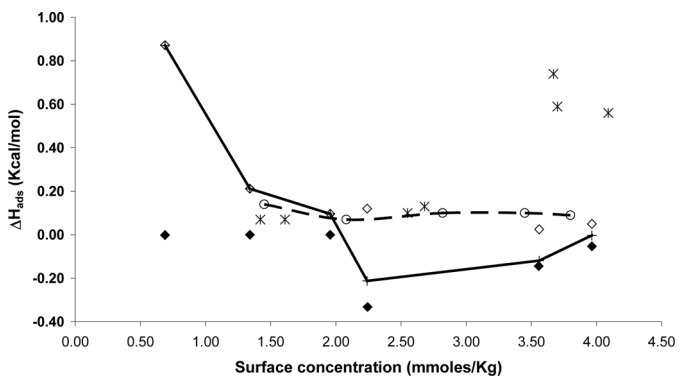


FIG. 7. Adsorption enthalpy (ΔH) of bovine serum albumin onto epoxy – (CH₂)₄ – sepharose in the presence of 1.0 M (NH₄)₂SO₄, pH 7.0 at different temperatures. (◊ – endothermic heat 296 K, ◆ – exothermic heat 296 K, + – net heat 296 K, ○ – 303 K, x – 308 K).

In an effort to build upon our prior work (15) we examined the role that temperature plays in HIC. In this paper, the adsorption of bovine serum albumin onto epoxy – (CH₂)₄ – Sepharose was extended to other temperatures. Shown in Fig. 7 are the heat of adsorption data obtained at 296 K (reported earlier (15) and included for convenience), 303 and 308 K. At the higher temperatures, no exothermic peaks were observed. Two possible reasons can be advanced for the disappearance of the exothermic peaks. The first possibility is that the exothermic and endothermic peaks overlap and a net endothermic heat is observed. The second possibility is that the exothermic peaks are not present at the higher temperatures. Exothermic peaks are indicative of attractive lateral interactions between adsorbed molecules and attractive interactions between the adsorbed molecules and the adsorbent surface. At 303 K, the magnitude of the endothermic heats (ΔH) appears to slightly decrease with an increase in protein adsorption, making plausible the possibility that exothermic heats (produced from favorable events) are reducing the magnitude of the resulting endothermic ΔH . Conversely at 308 K the magnitude of the endothermic ΔH_{ads} increases as the surface concentration of protein increases. This could be an indication of repulsive lateral interactions between adsorbed bovine serum albumin molecules. Valuable insight is obtained by correlating the ΔH data to the adsorption isotherms. Shown in Fig. 8 (results at 296 K reported earlier (15) and included for convenience) are the adsorption isotherms as function of temperature at 1.0 M (NH₄)₂SO₄. It is interesting to note that, at 303 K, the start of the region of rapidly increasing surface capacity occurs when the surface concentration of protein is approximately 104 to 138 mg/g of adsorbent. This corresponds closely to the surface concentration at which a slight decrease in ΔH is observed. These results reinforce the possible existence of exothermic heats under these

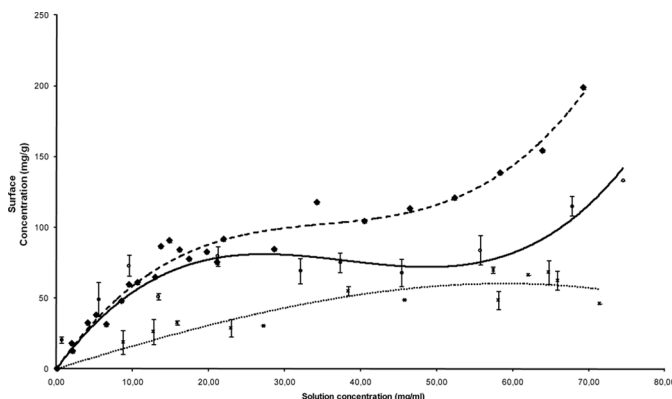


FIG. 8. Adsorption isotherms for bovine serum albumin onto epoxy- $(\text{CH}_2)_4$ -Sepharose in the presence of 1.0 M $(\text{NH}_4)_2\text{SO}_4$, pH 7.0 at different temperatures. (◆ - 296 K, ○ - 303 K, x - 308 K) (1). (The x axis is the equilibrium concentration of protein in units of milligrams of protein per milliliter of solution (mg/ml) and the y axis is the equilibrium surface concentration of protein in units of milligrams of protein per gram of adsorbent (mg/g)).

conditions. This behavior, as said before, is consistent with re-orientation and/or change in conformation of the adsorbed proteins. Furthermore, the disappearance of the region of rapidly increasing capacity at 308 K (Fig. 8) indicates the nonexistence of exothermic peaks at this temperature. From Fig. 8 it can also be seen that the surface concentration of protein is observed to decrease from 298 to 308 K, and the characteristic region of rapidly increasing capacity disappeared at 308 K. This strongly suggests an alteration of protein conformation with temperature. As temperature increases, the protein footprint in the adsorbed state will change. At the higher temperature, the protein will have a more open structure (bigger footprint) in the adsorbed state, leading to a lower quantity of protein adsorbed in the monolayer and consequently a decrease in capacity. Furthermore, with a bigger footprint the interaction of the protein with the surface is expected to be greater, thus minimizing the possibility of re-orientation and/or alteration of conformation of the adsorbed molecules. This is consistent with the disappearance of the region of rapidly increasing capacity at 308 K. Also, the significant positive value of ΔH at the higher temperature and surface concentration is indicative of repulsive interactions between adsorbed molecules and the establishment of only one monolayer. The trends observed in the enthalpy of adsorption data in this study are different from those reported by Huang and co-workers (32) in their study of the effect of temperature on the adsorption of α -chymotrypsinogen A and trypsinogen onto butyl and octyl-Sepharose. In prior publications (3,6,12) we have shown BSA adsorption onto an ion-exchange adsorbent is also entropically driven. This suggests the possibility that in certain applications, similar

adsorptive surface events may be present in HIC and ion-exchange. The work presented in this paper emphasizes the varying behaviors that systems can manifest, and the importance of characterizing each system independently.

CONCLUSIONS

This work examined some of the nonspecific effects on ion exchange and hydrophobic interaction adsorption processes. In ion exchange the interaction mechanism between two proteins (chymotrypsinogen and lysozyme) and two commercially available cation exchange resins (CMC and titanium oxide) at different pH values and salt concentrations was studied. In hydrophobic interaction, the effect of temperature on the adsorption mechanism of BSA onto epoxy- $(\text{CH}_2)_4$ -sepharose in presence of 1.0 M ammonium sulphate, pH 7.0 was analyzed.

Isotherm measurements were collected for chymotrypsinogen and lysozyme at pH 5 and pH 8. All measurements were conducted at 25°C. With respect to chymotrypsinogen, our results from this study indicated that the mechanism of adsorption may be dependent upon pH. At pH 8 the isotherms had an upward concave shape. Conversely at pH 5 the isotherms had a downward concave shape. The net surface charge for chymotrypsinogen was positive in both cases. The magnitude of the positive charge was greatest at pH 5. The lower charge density at pH 8 suggests the ion-exchange adsorptive mechanism may be very weak under these conditions. Consequently other non-specific adsorptive mechanisms may be driving chymotrypsinogen adsorption at the higher pH. As previously stated, at pH 5, chymotrypsinogen isotherms had a traditional downward concave shape. The affinity between the protein and the adsorbent appeared to be greater at the lower pH. Since the surface charge density of chymotrypsinogen was greater at pH 5, it is possible that the ion exchange mechanism may have been more prominent. Calorimetry measurements for chymotrypsinogen showed adsorption was endothermic at pH 8 and exothermic at pH 5. This data alone is indicative of different adsorptive mechanisms at each pH. Exothermic heats suggest the presence of favorable enthalpic events such as ion exchange. Endothermic heats indicate that protein adsorption is entropically driven. Entropically driven protein adsorption is usually a characteristic associated with hydrophobic interaction supports. Chen and co-workers (33) suggested the presence of hydrophobic interactions between ion-exchange resins and proteins at high salt concentration, or in a solution with a pH approaching the protein pI. Such was the case with chymotrypsinogen at pH 8. However, as argued in the discussion section, other processes may be present. In order to decide which of them are involved, a study of the dependence of heat of adsorption on the surface concentration should be done with a calorimeter having enough sensitivity to discern heat signals when the surface coverage is low.

With respect to lysozyme, the isotherms at pH 8 and pH 5 showed a strong affinity between the protein and the surface. Most of the isotherms exhibited a traditional Type I Langmuir shape. At the lower pH, the maximum protein surface concentration was reduced and the distribution coefficients in the linear region of the isotherms appeared to be smaller. Since lysozyme has a greater positive charge at pH 5, one would reasonably expect the affinity between the protein and adsorbent to be at least the same or perhaps greater. Calorimetry experiments showed lysozyme adsorption to be exothermic in all cases; however, the magnitude of the exothermic heat was reduced at the lower pH. A possible explanation for this may be the repulsive interactions between proteins in the vicinity of the adsorbent's surface; however, calorimetry measurements with greater heat signal detection capability are needed to verify this hypothesis in the presence of salt.

The affinity of chymotrypsinogen and lysozyme for TiO_2 was less when compared to CMC. This is significant because the zeta potential of titanium oxide is not that different from the measured zeta potential of CMC. The adsorption capacity of the TiO_2 adsorbent was never reached while the CMC adsorbent was fully saturated with protein. As previously stated, this may be indicative that the influence of entropic driving forces is greater in the presence of the carbonaceous stationary phase on the surface of carboxymethyl cellulose adsorbent.

Generally, it has been shown through linear HIC techniques that the adsorption process in hydrophobic interaction is entropically driven at lower temperatures and becomes enthalpically driven at higher temperatures (34). While calorimetric measurements of the adsorption of BSA onto epoxy- $(CH_2)_4$ -sepharose confirmed this behavior at low surface coverage, it also revealed different behavior at higher surface coverage, suggesting the alteration of the protein structure with temperature.

This paper illustrates the complexity of protein adsorption and the important role of non-ideal effects such as: protein-protein interactions on the adsorbent surface, protein reorientation and/or conformation change, and protein and adsorbent surface dehydration in the establishment of the adsorptive process. Theoretical and empirical models of adsorption equilibrium, under both linear and overloaded conditions should account for these non-specific effects, as well as the primary interactions. These non-ideal effects are the main reason why simulated isotherms can deviate from experimental isotherm data. However, because of the direct correlation between heat of adsorption data and isotherm measurements it would certainly be advantageous to use calorimetry data as a starting point in model selection or development. The use of such data provides valuable insight regarding the underlying driving forces for protein adsorption.

REFERENCES

1. Amersham Biosciences. (2007) *Ion Exchange Chromatography & Chromatofocusing, Principles and Methods*, AA Ed.; GE Healthcare.
2. Queiroz, J.A.; Tomaz, C.T.; Cabral, J.M.S. (2001) Hydrophobic interaction chromatography of proteins. *J. Biotechnol.*, 87: 143.
3. Thrash, M.E.; Phillips, J.M.; Pinto, N.G. (2004) An analysis of the interactions of BSA with an anion-exchange surface under linear and non-linear conditions. *Adsorption*, 10 (4): 299.
4. Brooks, C.A.; Cramer, S.M. (1992) Steric mass-action ion-exchange displacement profiles and induced salt gradients. *AIChE J.*, 38 (12): 1969.
5. Li, Y.; Pinto, N.G. (1995) Model for ion-exchange equilibria of macromolecules in preparative chromatography. *J. Chromatogr. A.*, 702: 113.
6. Raje, P.; Pinto, N.G. (1997) Combination of the steric mass action and non-ideal surface solution models for overload protein ion-exchange chromatography. *J. Chromatogr. A.*, 760: 89.
7. Roth, C.M.; Unger, K.K.; Lenhoff, A.M. (1996) Mechanistic model of retention in protein ion exchange chromatography. *J. Chromatogr. A.*, 726: 45.
8. Oberholzer, M.R.; Lenhoff, A.M. (1999) Protein adsorption isotherms through colloidal energetic. *Langmuir*, 15: 3905.
9. Bosma, J.C.; Wesselingh, J.A. (2004) Available area isotherm. *AIChE J.*, 50 (4): 848.
10. Gill, D.S.; Roush, D.J.; Willson, R.C. (1994) Adsorption heterogeneity and thermodynamic driving forces in anion-exchange equilibria of cytochrome-b(5). *J. Colloid Interf. Sci.*, 167: 1.
11. Bowen, W.R.; Hughes, D.T. (1993) Ion-exchange of proteins – A microcalorimetric study of the adsorption of bovine serum albumin on anion-exchange materials. *J. Colloid Interf. Sci.*, 158: 395.
12. Thrash, M.E.; Pinto, N.G. (2002) Characterization of enthalpic events in overloaded ion-exchange chromatography. *J. Chromatogr. A.*, 944 (1–2): 61.
13. Thrash, M.E.; Pinto, N.G. (2006) Incorporating water release and lateral protein interactions in modeling equilibrium adsorption for ion-exchange chromatography. *J. Chromatogr. A.*, 1126 (1–2): 304.
14. Bowen, W.R.; Pan, Li-Chun; Sharif, Adel O. (1998) Predicting equilibrium constants for ion exchange of proteins – A colloid science approach. *Colloid Surface A.*, 143: 117.
15. Esquibel-King, M.A.; Dias-Cabral, A.C.; Queiroz, J.A.; Pinto, N.G. (1999) Study of hydrophobic interaction adsorption of bovine serum albumin under overloaded conditions using flow microcalorimetry. *J. Chromatogr. A.*, 865: 111.
16. Dias-Cabral, A.C.; Pinto, N.G.; Queiroz, J.A. (2002) Studies on hydrophobic interaction adsorption of bovine serum albumin on polypropylene glycol sepharose under overloaded Conditions. *Separ. Sci. Technol.*, 37 (7): 1505.
17. Dias-Cabral, A.C.; Pinto, N.G.; Queiroz, J.A. (2003) Effect of salts and temperature on the adsorption of bovine serum adsorption of bovine serum albumin on polypropylene glycol-sepharose under linear and overloaded chromatographic conditions. *J. Chromatogr. A.*, 1018 (2): 137.
18. Dias-Cabral, A.C.; Ferreira, A.S.; Phillips, J.; Queiroz, J.A.; Pinto, N.G. (2005) The effects of ligand chain length, salt concentration and temperature on the adsorption of bovine serum albumin onto polypropylene glycol-sepharose. *Biomed. Chromatogr.*, 13 (8): 606.
19. Queiroz, J.A.; Garcia, F.A.P.; Cabral, J.M.S. (1995) Partitioning of chromobacterium viscosus lipases in aqueous two-phase systems. *J. Chromatogr. A*, 707: 137.
20. Steiner, R.; Tung, M. (1974) The self-association of chymotrypsinogen A. *Eur. J. Biochem.*, 44: 49.
21. Guiochon, G.; Shirazi, S.G.; Katti, A.M. (1994) *Fundamentals of Preparative and Nonlinear Chromatography*; Academic Press: Boston.

22. Oberholzer, M.R.; Lenhoff, A.M. (1999) Protein adsorption isotherms through colloidal energetic. *Langmuir*, 15: 3905.

23. Oberholzer, M.R.; Wagner, N.J.; Lenhoff, A.M. (1997) Grand canonical Brownian dynamics simulation of colloid adsorption. *J. Chem. Phys.*, 107: 9157.

24. Bernstein, F.C. (1977) Protein data bank-computer based archival file for macromolecular structures. *J. Mol. Biol.*, 112: 535.

25. Roth, C.M.; Lenhoff, A.M. (1995) Electrostatic and van der waals contributions to protein adsorption – Comparison of theory and experiment. *Langmuir*, 11: 3500.

26. Nemethy, G.; Scheraga, H.A. (1962) Structure of water and hydrophobic bonding in proteins. 3. Thermodynamic properties of hydrophobic bond in proteins. *J. Phys. Chem.*, 66 (10): 1773.

27. Lin, F.Y.; Chen, W.-Y.; Hearn, M.T.W. (2001) Microcalorimetric studies on the interaction mechanism between proteins and hydrophobic solid surfaces in hydrophobic interaction chromatography: Effects of salts, hydrophobicity of the sorbent, and structure of the protein. *Anal. Chem.*, 73 (16): 3875.

28. Perkins, T.W.; Mak, D.S.; Root, T.W.; Lightfoot, E.N. (1997) Protein retention in hydrophobic interaction chromatography. modeling variation with buffer ionic strength and column hydrophobicity. *J. Chromatogr. A.*, 766: 1.

29. Sophianopoulos, A.J.; Van Holde, K.E. (1964) Physical studies of Muramidase (Lysozyme) II. pH dependent dimerization. *J. Biol. Chem.*, 239: 2516.

30. Janusz, W.; Matysek, M. (2006) Coadsorption of Cd(II) and oxalate ions at the TiO₂/electrolyte solution interface. *J. Colloid Interf. Sci.*, 296: 22.

31. Duro, R.; Alvarez, C.; Martinez-Pacheco, R.; Gomez-Amoza, J.L.; Concheiro, A.; Souto, C. (1998) The adsorption of cellulose ethers in aqueous suspension of pyrantel pamoate: effect on zeta potential and stability. *Eur. J. Pharm. Biopharm.*, 45: 181.

32. Huang, H.-M.; Lin, F.-Y.; Chen, W.-Y.; Ruaan, R.-C. (2000) Isothermal titration microcalorimetric studies of the effect of temperature on hydrophobic interaction between proteins and hydrophobic adsorbents. *J. Colloid Interf. Sci.*, 229: 600.

33. Chen, W.Y.; Liu, Z.C.; Lin, P.-H.; Fang, C.I.; Yamamoto, S. (2007) The hydrophobic interactions of the ion-exchanger resin ligands with proteins at high salt concentrations by adsorption isotherms and isothermal titration calorimetry. *Sep. Purif. Technol.*, 54: 212.

34. Haidacher, D.; Vailaya, A.; Horvath, C. (1996) Temperature effects in hydrophobic interactions chromatography. *P. Natl. Acad. Sci. USA.*, 93: 2290.

35. Felder, R.M.; Rousseau, R.W. (2005) *Elementary Principles of Chemical Processes*, 3rd Ed.; John Wiley and Sons: New Jersey.

36. Zhang, X.; Samuelsson, J.; Janson, J.; Wang, C.; Su, A.; Gu, M.; Fornstedt, T. (2010) Investigation of the adsorption behavior of glycine peptides on 12% cross linked agarose gel media. *Journal of Chromatography A*, 1217: 1916.